Int. J. Adv. Res. Sci. Technol. Volume 10, Issue 12, 2022, pp.872-880.

IJARST

International Journal of Advanced Research in Science and Technology

journal homepage: www.ijarst.com

ISSN 2319 – 1783 (Print)

ISSN 2320 – 1126 (Online)

Identifying and Quantifying the Difference between Adenomatous Colon Polyps and Normal Colon Tissue from Clinical Histological Images

Abdelrahim Nasser Esgiar[1], Othman Omran Khalifa [2], Raouf Naguib[3], Ali Algaddafi [1], Laurence A. Gan Lim[4] and Alan Murray[5]*

[1] Department of Electrical and Electronic Engineering, Sirte University, Sirte, Libya

[2]International Islamic University Malaysia, Department of Electrical and Computer Engineering

[3]Liverpool Hope University, Liverpool, UK

[4]De La Salle University, Manila, Philippines

[5]Newcastle University, Newcastle upon Tyne, UK

****Corresponding author (e-mail: anasser6474@yahoo.co.uk)***

ARTICLEINFO

Article history:

Received 12 Dec 2022

Accepted 23 Dec 2022

Available online 25 Dec 2022

Keywords:

Colon polyp,
Microscopic image analysis,
Texture analysis,
Fractal dimension,
Lacunarity.

ABSTRACT

This study aimed to evaluate automated image analysis as a tool for differentiating normal tissue from adenomatous polyp lesions. Images of colon surgical pathology samples from 140 patients (70 normal subjects and 70 polyp subjects) were captured on a personal computer using an Olympus DP20 digital photomicrography apparatus mounted on an Olympus light microscope (trinocular) at 1200×1800 dots per inch resolution, with the high-power magnification of ×400. The complexity of image patterns was studied. In particular, image features of Fractal Dimension (FD) and Lacunarity (Lac) were extracted by using non-overlapping and sliding box-counting techniques. There were highly significant differences between the two clinical groups for both techniques, with polyp images in comparison with normal tissue images having significantly greater FD (1.83±0.04 v 1.73±0.08 $p<0.0001$) and significantly smaller Lac (0.28±0.08 v 0.42±0.12 $p<0.0001$) by using the non-overlapping box-counting method, and similar results by using the sliding box-counting method (1.86±0.09 v 1.78±0.08 $p<0.0001$, and 0.26±0.08 v 0.37±0.12 $p<0.0001$, respectively). These results encourage the use of computer automation, as normal colon tissue and adenomatous polyp tissue can be significantly differentiated.

PAPER-QR CODE

Citation: *Esgiar et al. Identifying and Quantifying the Difference between Adenomatous Colon Polyps and Normal Colon Tissue from Clinical Histological Images. Int. J. Adv. Res. Sci. Technol. Volume 10, Issue 12, 2022, pp.872-880.*

I. Introduction

It was reported in 2020 that colorectal cancer is the third leading cause of cancer deaths in both men and women in the USA [1,2], where approximately 5% of the population are diagnosed with cancer of the colon or rectum in their lifetime [3,4]. UK government data provided for England in 2021 shows a 5-year survival rate of only 59% [5], indicating that earlier detection is essential. This type of cancer is often preceded by the growth of polyps, which are tumours that build up in the walls of the colon. Most polyps are benign, but adenomatous polyps are strongly associated with colorectal cancer, and early detection and treatment can provide a major opportunity to save lives. Manual screening and pathological analysis of tissue are time-consuming and require the visual interpretation of complex images. This is usually based on subjective assessment techniques, which can lead to significant variations between observers. In some cases, even experienced pathologists or radiologists can misinterpret images and miss small polyp tumours [6,7]. Manual screening can be affected by operator fatigue, visual

habituation or differences in screening and diagnostic techniques. This is further compounded by the heterogeneity of some of the features. Therefore, the automation of polyp histology analysis could provide a valuable objective assessment, as well as contribute to a reduction in sources of error associated with subjective visual analysis.

Unfortunately, few studies have investigated the automatic classification of colon images, and scientific analyses comparing normal and polyp colon tissue has been seriously limited. A number of comparative studies have recently been published [8,9], exploring different techniques [10–15] for the identification and characterization of colonic polyps. As an aid to computer analysis, a study [16] showed that colon tissue fulfilled the mathematical definition of fractal structures. However, that study measured only the Fractal Dimension (FD) and no other fractal feature. A further study [14] examined colorectal adenomatous polyps, but only dysplastic mucosa was studied and was limited to 20 cases.

Table 1 presents a summary of the previous studies. Research in the classification of microscopic images of colonic mucosa has shown that texture features are useful when applied to medical image analysis [17,18]. Techniques studied for image analysis have included Haralick's features (entropy, correlation, inverse difference moment and angular second moment) [17,19–21], spatial domain [6,19,22], spectral domain [6,19,21,23], hyperspectral spatial domain [24–27], hybrid geometric feature space [28], kernel functions [29], as well as fractal dimension, mass dimension and Lacunarity (Lac) [16,22,30–36]. However, although some studies gave comparative statistical significance, very few provided actual data on the analysis of the measured features [22,30,31,34,37,38]. Among those studies with data, only two provided data on polyp analysis.

It can be seen in Table 1 that only one study [22] used both FD and Lac for colon cancer images, but it did not include polyp images, and the image samples were captured by Computed Tomography (CT) scans, and not by the more commonly used digital microscopy. Our previous study [30] used microscopy, but we had access only to limited data. In our current study, we used a much larger dataset, and more importantly, now include both normal and adenomatous polyp images. As this research was in collaboration with the University of the Philippines, it enabled us to significantly extend our research using data collected in a completely different environment, avoiding any potential differences or biases with locally collected data. We have also been able to extend our research technique to lacunarity features.

The aim of this study was therefore to extend our earlier work to a completely new clinical dataset and evaluate the added accuracy of combined techniques to improve automated histological image analysis. This paper was organised into the following sections. Section II presents the materials and methods, whereas section III shows the extraction of normal and polyp colon features using fractal analysis. The results and discussion presented in section IV and the final section which is section V conclude the paper.

II. Materials and Methods

1. *Histological Images*

The images used in this study were derived from slides of cases randomly selected from surgical pathology files of the Philippine General Hospital (PGH), Manila, Philippines, in 2007 and 2008. These were previously diagnosed as colonic adenocarcinoma, adenomatous polyps from the colon, as well as tumour-free colonic resection planes to serve as controls. The slides were routinely processed using a Sakura tissue processor and cut at eight μm using a standard microtome. All were stained with haematoxylin and eosin [39].

2. Ethical Approval

Ethical permission to study the colon images that were used in this research was granted by PGH. They were provided by our collaborating Consultant Pathologist, Dr. Jose Maria C. Avila, and they were retrieved from old archives of cases and are completely anonymous since the original slides and surgical pathology records had been discarded by the hospital.

3. *Imaging Modality and Preparation*

The images were captured using an Olympus DP20 digital photomicrography apparatus mounted on an Olympus light microscope (trinocular) at 1200×1800 dots per inch (dpi) resolution. A high-power magnification of ×400 was used for capturing the images on a personal computer, using a standard video grabber [39].

4. *Imaging Modality and Preparation*

140 colonic images were used for the analysis in this study. Two classes were considered, namely 'normal' and 'adenomatous polyps', with 70 image samples included in each class. These images gave a general representation of the infiltrative edge of the adenomatous polyps and of the thickness of the normal mucosa. Each image was resized down to 300×400 pixels and 8-bit grey level (monochromatic image) for the analysis, as shown in Fig 1.

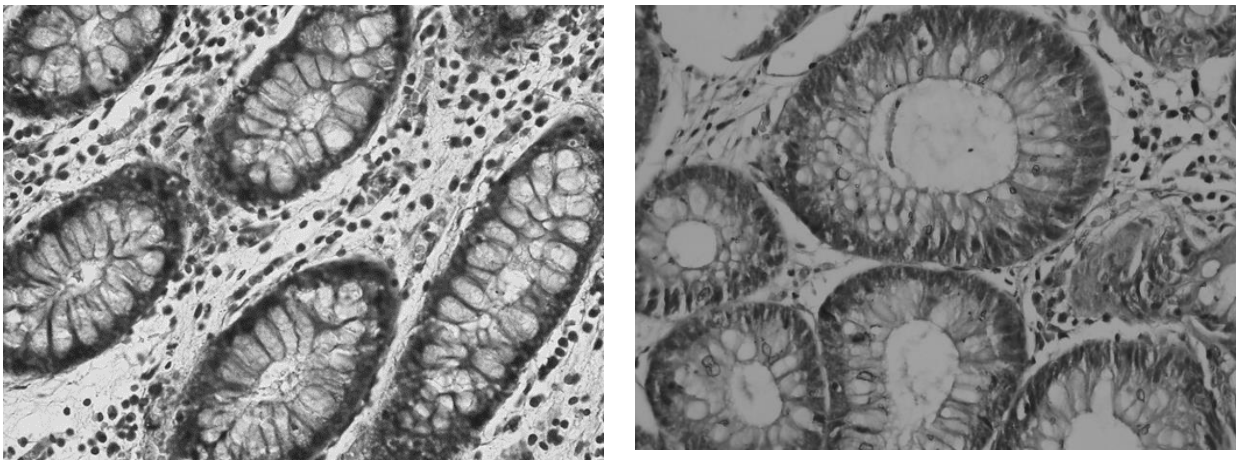

(A) **(B)**

Fig.1-Example of normal colon sample (A) and abnormal polyp sample (B)

III. Extraction of Normal and Polyp Colon Features Using Fractal Analysis:

Fractal analysis can provide quantitative parameters as quantifiers of complexity for the measurement of texture patterns. In this paper, we analyzed the FD and Lac of the colonic microscopic image samples.

Table 1. Summary of the published results comparing automated analyses of medical images using fractal analysis

Materials and Methods	[30] 2002	[22] 2009	[34] 2015	[36] 2020
Colon	Yes	Yes	Yes	No
Polyp	No	No	No	No
Image analysistechniques	Texture features from a grey-level co-occurrence matrix and fractal analysis	CT	Fractal analysis	Fractal analysis
Features	Correlation, Entropy and Fractal dimension (FD)	Fractal analysis	FD	FD
Numerical Results	Correlation (mean± SD): Normal=0.0326± 0.0075, Cancer=0.0510± 0.0097. Entropy (mean ±SD): Normal=1.01 ±0.15, Cancer=1.26± 0.11, FD (mean±SD): Normal=1.757±0.023, Cancerous=1.785±0.037, All p<0.0001	FD, Abundance and Lacunarity (Lac)	FD (mean): no SD Well-differentiated Cancer=1.431, Moderately differentiated=1.516, Weakly differentiated=1.669, Undifferentiated =1.741,p<0.001	FD (mean± SD): Normal =1.712±0.030 Cancer = 1.741±0.016, p<0.001

The box-counting technique was used to determine the self-similarity dimension [31]. In a self-similar structure, there is a relationship between the box-size scale factor, ε, and the number of boxes N(ε), into which the structure can be divided. This relationship of the FD is given by

$$FD = \ln(N(\varepsilon)) / \ln(1/\varepsilon) \quad (1)$$

Since fractals cannot be completely characterized by their FD, Lac can be used as a complementary measure to compensate for the lack of quantification of texture variations (inhomogeneities), or for deviation of a geometric structure from its translational invariance. In other words, lacunarity provides a tool to reveal 'gap' textures within an otherwise fractal distribution [40,41]. There is no formal definition of Lac and, indeed, there has been some controversy over how it should be measured [42]. Its concept and formulation were derived from differentiating two objects defined by the same fractal dimension but showing various visual textural patterns [43]. Therefore, Lac is considered a measure of perceived gaps, or holes, in the geometric structure of the image.

$$Lac_{\varepsilon} = (CV_{\varepsilon})^2 = (\sigma_{\varepsilon} / \mu_{\varepsilon})^2 \quad (2)$$

CV is the coefficient of variation for pixel distribution, μ is the standard deviation, σ is the mean of the data and ε is the scale factor applied to an object 'image'. In this study, we applied two box-counting techniques to extract the relevant features, from the ratio of increasing detail to the increasing scale factor (ε). These two techniques are described in the two following sections.

1). Estimating the fractal dimension of colon images using the non-overlapping box-counting approach

In this method, a non-overlapping regular square grid with a scale factor ε traversed the image to measure the box-counting dimension. The image was superimposed on a regular grid with a scale factor ε, and the number of grid boxes (windows) was counted. This gave a number, N(ε), with a value dependent on ε. Then we progressively changed ε to smaller sizes and counted the corresponding N(ε).

Next, we plotted the distribution log(N(ε))/log(1/ε) for each image, fitted a straight (regression) line to the points, and measured its slope (equation 1), to give the box-counting dimension. Each part of the image was sampled only once for each box size and repeated until the whole surface area of the image had been traversed [43,44].

2). Estimating the fractal dimension of colon images using the sliding-box approach

The following settings were developed according to the recommendations of the FracLac user manual [44]. The size of the series about the sliding-box technique was set to decrease linearly from a maximum box size of 41% of the entire image or Region of Interest (ROI) size to a minimum size of 3×3 pixels. The square box of size ε was slid over the entire image so that it overlapped with each movement. The sliding-box scan then counts the number of pixels inside the box and the number of boxes, N(ε), slide the boxes horizontally by a fixed number of pixels (x) and then recounts the pixels that fell on the box, and the number of boxes, N(ε). At the end of each row, the box was slid down by a fixed number of pixels (y), and the row was scanned again in the same way until the entire image had been scanned. Then we progressively changed ε to smaller sizes and counted pixels that fell on the box and the corresponding N(ε). This process was repeated for each box size until the entire area of the image had been scanned using each ε. Next, we plotted log(N(ε))/log(1/ε), fitted a straight (regression) line to the points, and measured its slope (equation 1). This technique differs from a regular box-counting scan in which all boxes are of a fixed size and are laid on a non-overlapping grid [43,44]. The non-overlapping grid can be seen as a special case of the sliding-box algorithm, with horizontal and vertical increments equal to the scale factor, ε.

3). Computing lacunarity scaling of colon images using the non-overlapping and the sliding-box scan approaches

For both non-overlapping and sliding-box counting, Lac was determined from the probability distribution for pixel 'mass distribution'. Lacunarity at a particular was labelled, and calculated as the variation in pixel density at different box sizes, using the CV for pixel distribution as in equation (2) [43,44]. Lac varied with the size of the sampling unit. Thus, in order to arrive at a single number, the values were summarised as the mean, overall scale factors, ε[43,44].

4). Statistical analysis

The statistical analysis of the extracted features (Table 2, Figures 2-4) was performed using the Minitab 17 software, including mean, Standard Deviation (SD) and Standard Error of the mean (SE). An analysis of variance (ANOVA) was performed to analyze for significant differences between the normal and adenomatous polyp lesions. We also evaluated several classification models using logistic regression, including a combination of the four predefined features: Fractal Dimension using the Box-Counting technique (FdB) and Sliding-Box technique (FdS), and Lacunarity using the Box-Counting technique (LacB) and Sliding-Box technique (LacS), as follows:

- Model_1: FdB
- Model_2: FdS
- Model_3: LacB
- Model_4: LacS
- Model_5: FdB + LacB
- Model_6: FdS + LacS
- Model_7: LacB + LacS
- Model_8: FdB + FdS
- Model_9: FdB + LacB + LacB + LacS

Each model was evaluated by using the Area Under Curve (AUC) and the Receiver Operating Characteristic (ROC) curves as global performance criteria. In addition, the Classification Accuracy (ACC) of each model was calculated. The ACC is the ratio of the number of correct classifications relative to the total number of classifications. To avoid any overfitting problems, all models were evaluated using a 10-fold cross-validation, repeated 300 times.

LacB and FdB denote the Lacunarity and Fractal dimension, respectively, using the non-overlapping box-counting method. LacS and FdS denote the Lacunarity and Fractal dimension, respectively, using the sliding-box method. t & p denote t and p-values which are a statistical measure of the results evidence against the null hypothesis.

IV. Results and Discussion

It was reported

1). Analysis of differences between normal and patient groups: Table 2 gives the results and statistical analysis for the four primary comparisons, providing the statistical comparison of the difference between the normal and adenomatous polyp groups.

2). Analysis of differences between the non-overlapping box-counting and sliding-box methods:
In Table 3, an analysis of the differences in Lac and FD for the non-overlapping box-counting (B) and sliding-box (S) techniques is given.

3). Comparison between the non-overlapping box-counting and sliding-box methods:

Fig 2 shows the relationships between the non-overlapping box-counting and sliding-box techniques for the FD and Lac parameters, respectively, for all normal and adenomatous polyp patient samples. Both relationships are highly significantly correlated: FD at r2=0.973, p<0.0001 and Lac at r2= 0.981, p<0.0001).

4). Separation of normal subjects from patients:

Fig3 shows the 95% CI group separation for both FD (p<0.0001) and Lac (p<0.0001) on the non-overlapping box-counting method. This highlights how well the two groups are differentiated using this method.

5). Combined fractal dimension and Lacanalysis:

Fig4 presents a plot from the non-overlapping box-counting method showing the relationship between fractal dimension and Lac, separately, for the normal colon (r2=0.867, p<0.0001) and abnormal adenomatous polyp (r2=0.764, p<0.0001) subjects.

6). Distribution of FD and Lac for normal colon and abnormal polyp images:

Fig5 shows the distributions of FD and Lac across all 70 normal and 70 polyp subjects, for both non-overlapping box-counting methods. Based on the results reported in Tables 2 and 3, and Figures 2-5, the following significant results of the work can be emphasised: First, the fractal dimension in the case of adenomatous polyps was significantly larger than in the case of normal tissue, based on both the non-overlapping box-counting and sliding-box techniques. Also, the Lac for adenomatous polyps was significantly lower than for normal tissue, again based on both techniques. Furthermore, the non-overlapping box-counting technique yielded significantly different values than the sliding-box technique. Second, the non-overlapping box-counting technique yielded significantly smaller values for fractal dimension, but significantly larger values for Lac, compared with the sliding-box technique.

Table 2. Analysis of differences between box-counting and sliding-box methods

Population	Features	95% CI fordifference	t-value	p-value
Normal	LacB, LacS	(0.0512, 0.0564)	37.5	<0.0001
Adenomatous polyp	LacB, LacS	(0.0221, 0.0274)	42.4	<0.0001
Normal	FdB, FdS	(-0.0480, -0.0424)	-33.7	<0.0001
Adenomatous polyp	FdB, FdS	(-0.0345, -0.0289)	-36.8	<0.0001

Nonetheless, as noted above, the non-overlapping box-counting technique resulted in a more pronounced differentiation between normal and adenomatous polyp tissue. Third, there was an inverse relationship between FD and Lac, which is in line with the underlying theory of fractal analysis [41,45].

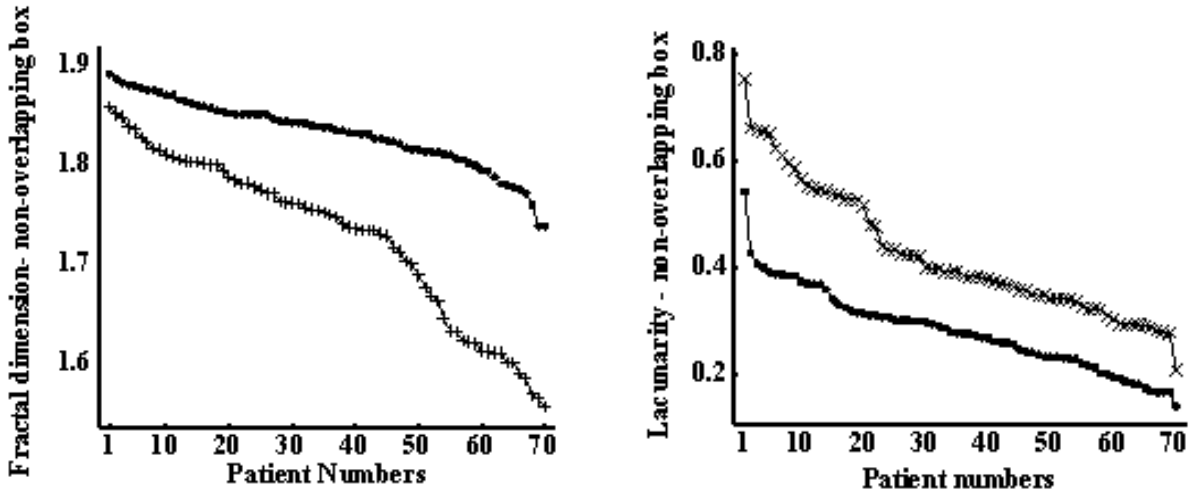

Fig.2-Non-overlapping box-counting technique showing the distributions of fractal dimension (left) and lacunarity (right) across all 140 (70 normal colon subjects and 70 abnormal patients)[(•) denotes normal subjects;(+) denotes abnormal adenomatous polyp subjects].

7). Performance comparison of selected classification models. Fig 6 shows the AUC results of the proposed 9 models, using different combinations of FD and Lac features, measured by both the non-overlapping box-counting and sliding-box methods. An AUC ranges from 0 to 1. Values greater than 0.7 refer to acceptable

discrimination between patients with and without the disease and values greater than 0.8 is considered excellent [46]. The results show that the models based on FD features outperform those based on Lac features. Concerning the evaluation of the classification models, we noticed that the models based on FD features slightly outperformed those based on Lac features. The best AUC results were obtained by the model combining FD features calculated from both sliding-box and non-overlapping box-counting techniques (AUC=0.85, ACC=10.06), as illustrated in Fig 6.

Table 3. Analysis of differences between the normal and adenomatous polyp groups

Features	Normal Mean ±SD	Polyps Mean ±SD	Normal SE Mean	Polyp SE Mean	95% CI for difference	t	p
LacB	0.424 ±0.119	0.283±0.077	0.014	0.0092	(0.108, 0.175)	7.39	<0.0001
LacS	0.371 ±0.117	0.258±0.078	0.014	0.0094	(0.078, 0.147)	7.29	<0.0001
FdB	1.729±0.082	1.832±0.035	0.0099	0.0041	(-0.124, -0.082)	-7.97	<0.0001
FdS	1.775±0.0832	1.864±0.092	0.0099	0.0041	(-0.111, -0.068)	-7.73	<0.0001

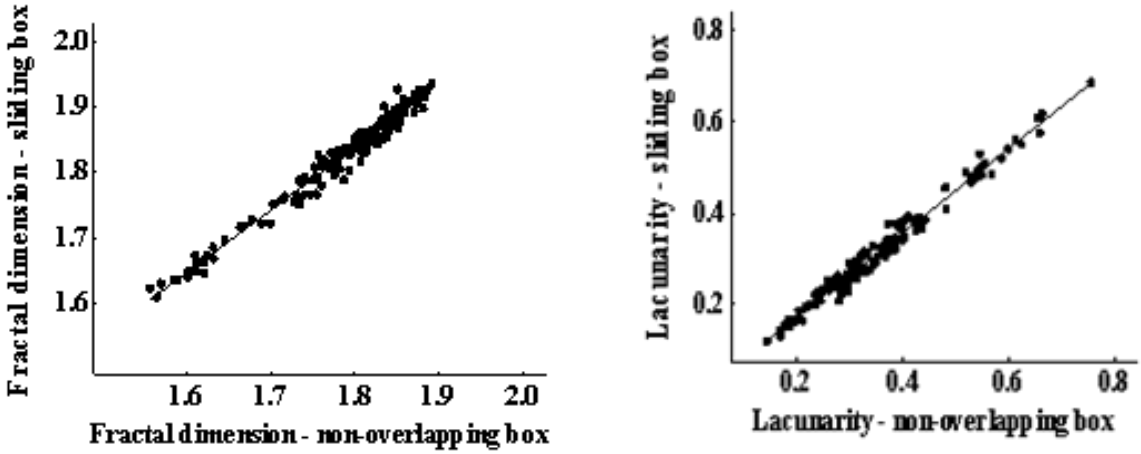

Fig. 3- Relationships between the sliding-box and non-overlapping box methods for fractal dimension (left) and lacunarity (right).

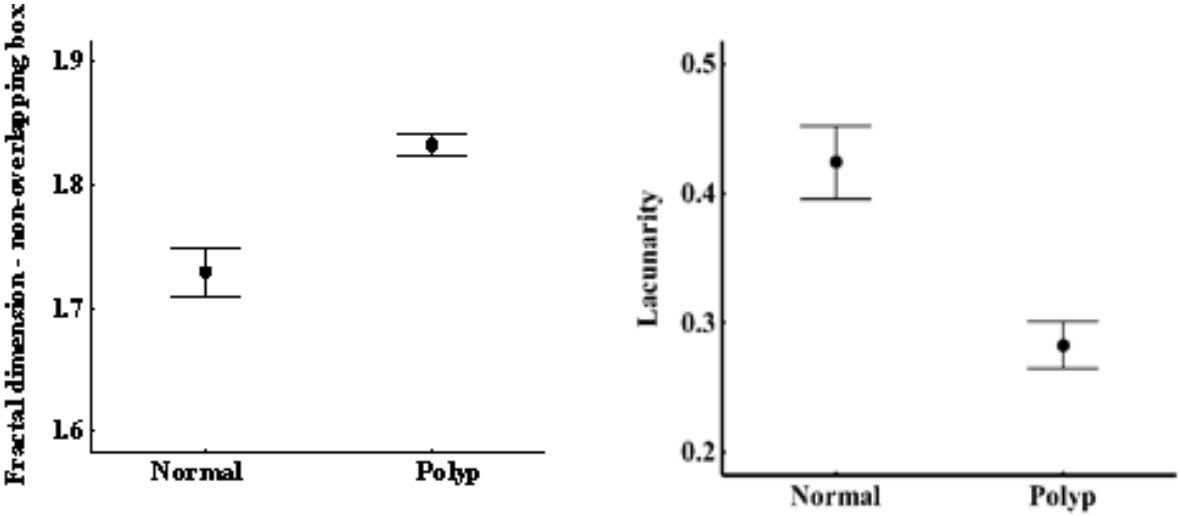

Fig.4-Non-overlapping box-counting techniques showing the 95% confidence interval with group separation for fractal dimension (left) and lacunarity(right).

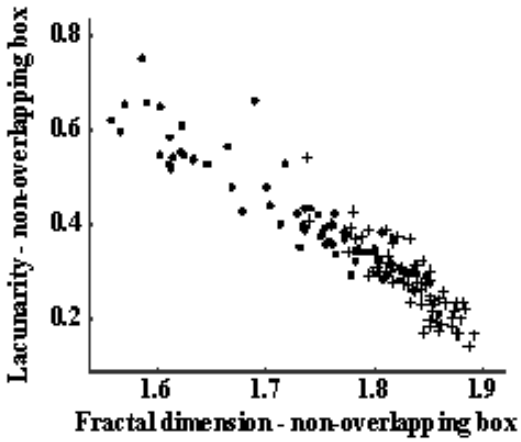

Fig.5-Non-overlapping box-counting technique showing the relationship between fractal dimension and lacunarity [(•) denotes normal subjects; (+) denotes abnormal adenomatous polyp subjects].

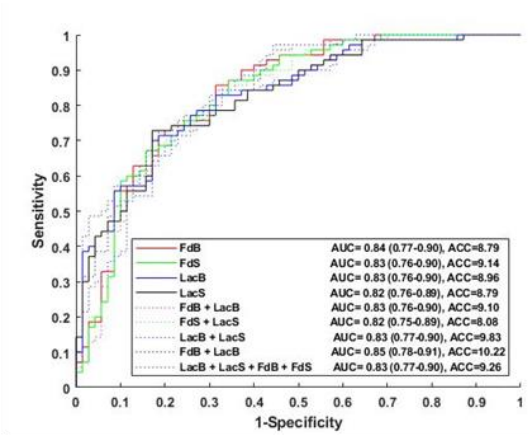

Fig.6-ROC curves for the 9 classification models.

V. Conclusion

This study has demonstrated that fractal analysis parameters result in highly significant differences between normal and adenomatous polyp colonic mucosa images. Since the fractal analysis parameters significantly differ for normal tissue and adenomatous polyps, this study, therefore, provides evidence for the value of fractal dimension and lacunarity features for effectively differentiating between these two clinical groups. We believe that the use of accurate and robust features can significantly contribute to more reliable automated diagnostic measurements, leading to an enhanced improvement in the detection of adenomatous colon polyps.

Conflicts of Interest

There are no conflicts of interest.

Acknowledgements

The authors wish to acknowledge the valuable clinical contribution of Dr Jose Maria "Joey" Avila, who unfortunately succumbed to Covid-19 and sadly passed away in April 2021. Dr Avila was a brilliant histopathologist and the head of Makati Medical Centre's Department of Pathology and Laboratories in the Philippines. He provided the research team with the pathology images used in this study and, if it had not been for his death, he would have been one of our co-authors.

References

1. Alshammari SA, Alenazi HA, Alshammari HS. Knowledge, attitude and practice towards early screening of colorectal cancer in Riyadh. J Family Med Prim Care 2020;9:2273–80. https://doi.org/10.4103/jfmpc.jfmpc_290_20.
2. Siegel RL, Miller KD, Goding Sauer A, Fedewa SA, Butterly LF, Anderson JC, et al. Colorectal cancer statistics, 2020. CA: A Cancer Journal for Clinicians 2020;70:145–64.
3. American Cancer Society. Colorectal cancer facts & figures 2014-2016. 2014.
4. Siegel RL, Miller KD, Fedewa SA, Ahnen DJ, Meester RGS, Barzi A, et al. Colorectal cancer statistics, 2017. CA: A Cancer Journal for Clinicians 2017;67:177–93.
5. Baker C. Cancer statistics (England), Research Briefing. House of Commons Library 2021.
6. Fu JJC, Yu Y-W, Lin H-M, Chai J-W, Chen CC-C. Feature extraction and pattern classification of colorectal polyps in colonoscopic imaging. Computerized Medical Imaging and Graphics: The Official Journal of the Computerized Medical Imaging Society 2014;38:267–75.
7. Pooler BD, Kim DH, Weiss JM, Matkowskyj KA, Pickhardt PJ. Colorectal polyps were missed with optical colonoscopy despite previous detection and localization with CT colonography. Radiology 2016;278:422–9. https://doi.org/10.1148/radiol.2015150294.
8. Rathore S, Hussain M, Ali A, Khan A. A recent survey on colon cancer detection techniques. IEEE/ACM Transactions on Computational Biology and Bioinformatics 2013;10:545–63.
9. Malik J, Kiranyaz S, Kunhoth S, Ince T, Al-Maadeed S, Hamila R, et al. Colorectal cancer diagnosis from histology images: A comparative study. ArXiv 2019.
10. Hamilton PW, Allen DC, Watt PC, Patterson CC, Biggart JD. Classification of normal colorectal mucosa and adenocarcinoma by morphometry. Histopathology 1987;11:901–11.
11. Bibbo M, Michelassi F, Bartels PH, Dytch H, Bania C, Lerma E, et al. Karyometric marker features in normal-appearing glands adjacent to human colonic adenocarcinoma. Cancer Res 1990;50:147–51.
12. Thompson D, Bartels PH, Bartels HG, Hamilton PW, Sloan JM. Knowledge-guided segmentation of colorectal histopathologic imagery. Analytical and Quantitative Cytology and Histology 1993;15:236–46.
13. McNitt-Gray MF, Huang HK, Sayre JW. Feature selection in the pattern classification problem of digital chest radiograph segmentation. IEEE Transactions on Medical Imaging 1995;14:537–47.
14. Hamilton PW, Bartels PH, Thompson D, Anderson NH, Montironi R, Sloan JM. Automated location of dysplastic fields in colorectal histology using image texture analysis. The Journal of Pathology 1997;182:68–75.
15. Babu T, Gupta D, Tripty S, Hameed S. Prediction of normal & grades of cancer on colon biopsy images at different magnifications using Minimal Robust Texture & Morphological Features. Indian Journal of Public Health

Research & Development 2020;11:695. https://doi.org/10.37506/v11/i1/2020/ijphrd/193905.
16. Cross SS, Bury JP, Silcocks PB, Stephenson TJ, Cotton DW. Fractal geometric analysis of colorectal polyps. The Journal of Pathology 1994;172:317–23.
17. Esgiar AN, Naguib RN, Sharif BS, Bennett MK, Murray A. Microscopic image analysis for quantitative measurement and feature identification of normal and cancerous colonic mucosa. IEEE Transactions on Information Technology in Biomedicine: A Publication of the IEEE Engineering in Medicine and Biology Society 1998;2:197–203.
18. Cicchi R, Kapsokalyvas D, De Giorgi V, Maio V, Van Wiechen A, Massi D, et al. Scoring of collagen organization in healthy and diseased human dermis by multiphoton microscopy. Journal of Biophotonics 2010;3:34–43.
19. Shuttleworth JK, Todman AG, Naguib RNG, Newman BM, Bennett MK. Colour texture analysis using co-occurrence matrices for classification of colon cancer images. IEEE CCECE2002. Canadian Conference on Electrical and Computer Engineering. Conference Proceedings (Cat. No.02CH37373), vol. 2, 2002, p. 1134–9 vol.2.
20. Masood K, Rajpoot N. Texture based classification of hyperspectral colon biopsy samples using CLBP. 2009 IEEE International Symposium on Biomedical Imaging: From Nano to Macro, 2009.
21. Jiao L, Chen Q, Li S, Xu Y. Colon cancer detection using whole slide histopathological images. In: Long M, editor. World Congress on Medical Physics and Biomedical Engineering May 26-31, 2012, Beijing, China, Berlin, Heidelberg: Springer; 2013, p. 1283–6.
22. Goh V, Sanghera B, Wellsted DM, Sundin J, Halligan S. Assessment of the spatial pattern of colorectal tumour perfusion estimated at perfusion CT using two-dimensional fractal analysis. European Radiology 2009;19:1358–65.
23. Tjoa MP, Krishnan S. Texture-based quantitative characterization and analysis of colonoscopic images. Proceedings of the Second Joint 24th Annual Conference and the Annual Fall Meeting of the Biomedical Engineering Society.Engineering in Medicine and Biology 2002:1090–1.
24. Woolfe F, Maggioni M, Davis G, Warner F, Coifman R, Zucker S. Hyper-spectral microscopic discrimination between normal and cancerous colon biopsies. IEEE Transactions on Medical Imaging 1999;99:1–10.
25. Rajpoot KM, Rajpoot NM. Wavelet based segmentation of hyperspectral colon tissue imagery. 7th International Multi Topic Conference, 2003. INMIC 2003., 2003, p. 38–43.
26. Rajpoot K, Rajpoot N. SVM optimization for hyperspectral colon tissue cell classification. Lecture Notes in Computer Science 2004;3217:829–37.
27. Akbari H, Halig LV, Zhang H, Wang D, Chen ZG, Fei B. Detection of cancer metastasis using a novel macroscopic hyperspectral method. Proceedings of SPIE 2012;8317:831711.
28. Rathore S, Hussain M, Khan A. Automated colon cancer detection using hybrid of novel geometric features and some traditional features. Computers in Biology and Medicine 2015;65:279–96.
29. Chen Z-Y, Li JA Multiple kernel support vector machine scheme for simultaneous feature selection and rule-based classification. 2007. https://doi.org/10.1007/978-3-540-71701-0_44.
30. Esgiar AN, Naguib RNG, Sharif BS, Bennett MK, Murray A. Fractal analysis in the detection of colonic cancer images. IEEE Transactions on Information Technology in Biomedicine: A Publication of the IEEE Engineering in Medicine and Biology Society 2002;6:54–8.
31. Marghani KA, Dlay SS, Sharif BS, Sims AJ. Morphological and texture features for cancer tissues microscopic images. Medical Imaging 2003: Image Processing, vol. 5032, SPIE; 2003, p. 1757–64.
32. Esgiar AN, Chakravorty PK. Fractal based classification of Colon cancer tissue images. 2007 9th International Symposium on Signal Processing and Its Applications, 2007, p. 1–4.
33. Franzén LE, Hahn-Strömberg V, Edvardsson H, Bodin L. Characterization of colon carcinoma growth pattern by computerized morphometry: definition of a complexity index. International Journal of Molecular Medicine 2008;22:465–72.
34. Streba L, ForȚofoiu MC, Popa C, Ciobanu D, Gruia CL, Mogoantă SȘ, et al. A pilot study on the role of fractal analysis in the microscopic evaluation of colorectal cancers. Romanian Journal of Morphology and Embryology = Revue Roumaine De Morphologie Et Embryologie 2015;56:191–6.
35. Barucci A, Farnesi D, Ratto F, Pelli S, Pini R, Carpi R, et al. Fractal-radiomics as complexity analysis of CT and MRI cancer images. 2018 IEEE Workshop on Complexity in Engineering (COMPENG), 2018, p. 1–5. https://doi.org/10.1109/CompEng.2018.8536249.
36. Qin J, Puckett L, Qian X. Image based fractal analysis for detection of cancer cells, IEEE Computer Society; 2020, p. 1482–6.
37. Panigrahy C, Seal A, Mahato NK. Image texture surface analysis using an improved differential box counting based fractal dimension. Powder Technology 2020;364:276–99. https://doi.org/10.1016/j.powtec.2020.01.053.
38. Panigrahy C, Seal A, Mahato NK. Quantitative texture measurement of gray-scale images: Fractal dimension using an improved differential box counting method. Measurement2019;147:106859. https://doi.org/10.1016/j.measurement.2019.106859.
39. Gan Lim LA, Naguib R, Dadios EP, Avila JMC. Image classification of microscopic colonic images using textural properties and KSOM. International Journal of Biomedical Engineering and Technology 2010;3:308–18.
40. Gefen Y, Meir Y, Mandelbrot BB, Aharony A. Geometric implementation of hypercubic lattices with noninteger dimensionality by use of low lacunarity fractal lattices. Physical Review Letters 1983;50:145–8.
41. Filho MNB, Sobreira FJA. Accuracy of lacunarity algorithms in texture classification of high spatial resolution images from urban areas. International Archives of Photogrammetry, Remote Sensing and Spatial Information Sciences 2008:417–22.
42. Theiler J. Lacunarity in a best estimator of fractal dimension. Physics Letters A 1988;133:195–200.
43. Karperien A, Ahammer H, Jelinek HF. Quantitating the subtleties of microglial morphology with fractal analysis. Frontiers in Cellular Neuroscience 2013;7:3.
44. Karperien A. FracLac for imageJ – FracLac advanced user's manual, Charles Sturt University Australia 2004.
45. Soares F, Janela F, Pereira M, Seabra J, Freire MM. 3D lacunarity in multifractal analysis of breast tumor lesions in dynamic contrast-enhanced magnetic resonance imaging. IEEE Transactions on Image Processing: A

Publication of the IEEE Signal Processing Society 2013;22:4422–35.

46. Mandrekar JN. Receiver operating characteristic curve in diagnostic test assessment. Journal of Thoracic Oncology: Official Publication of the International Association for the Study of Lung Cancer 2010;5:1315–6.